The Central kpc of Starbursts and AGN
ASP Conference Series, Vol. xxx, 2001
J. H. Knapen, J. E. Beckman, I. Shlosman, and T. J. Mahoney

Star Formation in Starbursts and Active Galactic Nuclei

Claus Leitherer

Space Telescope Science Institute[1], 3700 San Martin Drive, Baltimore, MD 21218, USA

Abstract. An overview of our current understanding of star formation in starburst galaxy centers and in active galactic nuclei is presented. On kpc-wide scales the average star formation density depends on the mean surface density of the molecular gas. Observations at higher spatial resolution indicate structure at sizes down to a few pc. These structures are identified as very luminous star clusters, which may be the smallest unit of star formation in starbursts. The most luminous galaxies whose energy production is dominated by a starburst have luminosities of about 2×10^{12} $L_\odot$. At higher luminosities, active galactic nuclei always dominate the energy release. There is clear evidence for a close association of the starburst and AGN phenomenon. While a causal relation between starbursts and AGNs, if it exists, has not yet been established observationally, the ubiquity of starbursts around many AGNs suggests a common triggering and feeding mechanism.

1. Introduction

Highly energetic activity in the centers of some galaxies has been known for almost a century (e.g., Slipher 1917). Yet the source of the activity remained elusive even as late 1963 when Lynds & Sandage summarized the observational evidence for an explosion in the (now) proto-typical starburst galaxy M82: "*The nature of the initial explosion in the central regions of M82 is an enigma. But M82 may be the first recognized case of a high energy explosion originating in the central regions of a galaxy, and as such may provide features required for a general explanation of many extragalactic radio sources.*" Star formation as a source for the observed phenomena in the centers of galaxies like M82 or NGC 253 was later invoked, e.g., by Rieke & Low (1975).

Balzano (1983) quantified the statistical properties of galaxies with *starburst* nuclei, a term coined by Weedman et al. (1981). Galaxies with starburst nuclei represent about 3% of the field galaxies with absolute photographic magnitudes $-17.7 > M_P > -22.5$. In terms of star formation, Heckman (1997) estimated that about 25% of the massive-star formation in the local universe occurs in starbursts as opposed to normal disk and irregular galaxies. This percentage is likely to increase with redshift and may approach 100% in the early universe.

---

[1]Operated by AURA, Inc., for NASA under contract NAS5-26555

This review is an attempt to give an overview of our current understanding of the starburst phenomenon and its relation to active galactic nuclei (AGN). I will use the working definition of a starburst as a kpc or smaller sized region with highly elevated, recent star formation density. As an example I mention M82, whose star formation rate as derived from the infrared (IR) luminosity in the central kpc is of order 1 $M_\odot$ yr^{-1} (Rieke 1991). This is comparable to the total star formation rate in the disk of our Milky Way but a factor of 100 higher in terms of star formation density. Galaxies hosting starbursts are a diverse group. The best studied galaxy types with starburst nuclei are ultraviolet-excess objects of the Markarian list (Balzano 1983), H II galaxies (Terlevich et al. 1991), and IR-luminous galaxies (Soifer et al. 1987).

The outline of the paper is as follows. First, I will review the overall star formation properties of starburst galaxies (Section 2). Then I will zoom in by a factor of ∼100 and discuss the detailed starburst morphology on scales of pc and tens of pc in Section 3. Many starburst regions are deeply embedded in dust. In Section 4 I discuss how we can unveil the underlying stellar population and the implications of dust obscuration for the derived star formation rates. The starburst-AGN connection is reviewed in Section 5. Finally, I address the energetic significance of starbursts and AGN in luminous galaxy hosts from recent ISO results (Section 6).

2. Global Star Formation: kpc Scales

Schmidt (1959) proposed a simple scaling law between the star formation rate and the gas density of the interstellar medium (ISM). This relation was shown by Kennicutt (1998) to be applicable to starburst galaxies as well. Combining the star formation rate surface densities, $\Sigma_{\rm SFR}$, and the surface densities of the molecular gas, $\Sigma_{\rm Gas}$, of normal disk galaxies and of starburst galaxies, a tight correlation between $\Sigma_{\rm SFR}$ and $\Sigma_{\rm Gas}$ over four decades is found:

$$\Sigma_{\rm SFR} \propto \Sigma_{\rm Gas}^{1.4\pm0.15} \qquad (1)$$

Fig. 1 shows this relation. Remarkably, the data are consistent with a single Schmidt law extending over the whole surface density range from normal spiral galaxies to starburst regions. There are two important restrictions to the applicability of Fig. 1. First, the relation was derived by averaging over surfaces of order 1 kpc^2 for starbursts. This *global* relation cannot be extrapolated to scales smaller than hundreds of pc. It is well-known that star formation occurs on much smaller scales, and the connection between the larger and the smaller scales is not obvious (Elmegreen 1999). Indeed we expect larger and larger deviations from eq. (1) for smaller and smaller star formation regions. Second, the relation will fail completely below a certain threshold surface density (Martin & Kennicutt 2001). This threshold may be related to the threshold for large-scale gravitational instability.

Fig. 1 can be taken as empirical evidence that the star formation rates (SFR) in starbursts are higher because the central gas densities are higher. Consequently, processes capable of increasing the central gas density can potentially trigger a starburst. For the gas to flow into the nucleus, angular momentum loss

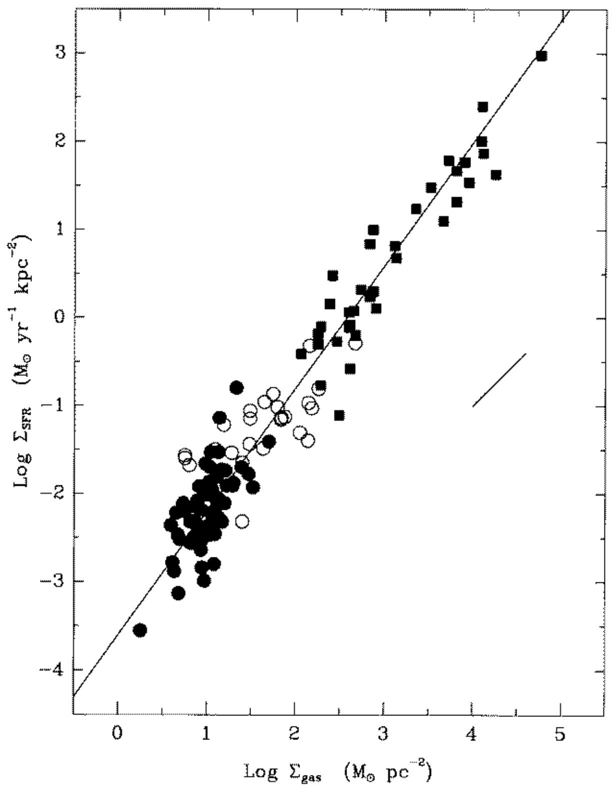

Figure 1. Composite star formation law for normal disk (filled circles) and starburst (squares) galaxies. Open circles: centers of normal disk galaxies. The line is a least-squares fit with index $n = 1.4$. From Kennicutt (1998).

of the extra-nuclear gas must occur. Possible mechanisms include interaction-induced angular momentum loss by gravitational torque and dissipation (e.g., Mihos & Hernquist 1996). Since the seminal work of Tinsley & Larson (1978) it has been known that star formation is enhanced in interacting galaxies. The most extreme cases in terms of luminosity ($L \geq 10^{12}$ $L_\odot$) and therefore SFR are ultraluminous infrared galaxies (ULIRG). Almost all ULIRGs are in interacting or merging systems (Sanders 1997). Alternatively, bars induce angular momentum loss with subsequently central gas flows (Shlosman, this conference).

What are the observed total SFRs in starburst galaxies? A far-IR selected sample of starburst galaxies gives the least biased census of the global star formation since selection effects due to dust obscuration are avoided. The far-IR luminosity traces the ionizing and non-ionizing radiation from young OB stars which is absorbed by dust and re-emitted at a peak wavelength of ~60 μm. It is thus sensitive to the star formation history over tens of Myr. If the entire stellar radiation is converted and if a power law stellar initial mass function (IMF) with $\alpha = 2.35$ between 1 and 100 $M_\odot$ is assumed, the relation between far-IR

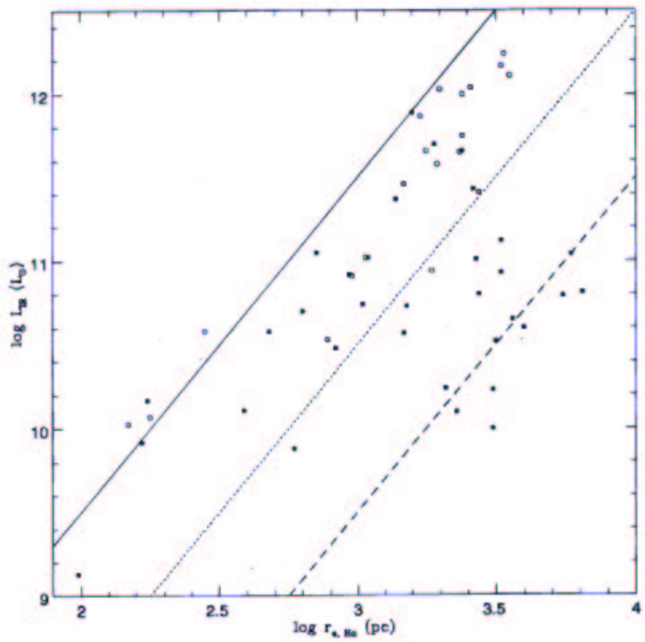

Figure 2. IR luminosity vs. size of the Hα emitting region for a sample of far-IR selected starburst galaxies. The three diagonal lines represent constant IR luminosities per unit area of 10^{11}, 10^{10}, and 10^{9} $L_\odot$ kpc^{-2}, respectively. From Lehnert & Heckman (1996).

luminosity (in $L_\odot$) and SFR (in $M_\odot$ yr^{-1}) is:

$$\mathrm{SFR} \approx 1 \times 10^{-10} L_{\mathrm{IR}} \tag{2}$$

(Leitherer et al. 1999; their Fig. 46 at 20 Myr). Note that the conversion factor becomes 7×10^{-10} for an IMF slope of 3.3. Other uncertainties in the conversion to star formation rates are introduced by the fraction of far-IR emission contributed by an older disk population and by the amount of radiation emitted by polycyclic aromatic hydrocarbon in the mid-IR. Therefore, star formation rates for *individual* galaxies may have large uncertainties.

Lehnert & Heckman (1996) utilized a large sample of IR-selected starburst galaxies to derive star-formation rates from the IR and to establish correlations with host galaxy properties. Fig. 2 shows the far-IR luminosities. With eq. (2), the luminosities translate into SFRs of up to a few hundred $M_\odot$ yr^{-1}. Since an IR-selected sample is biased towards the highest luminosities, the star formation rates are close to the largest rates observed in starburst galaxies. Conversely, the low-luminosity cut-off results from the sample being flux limited. Less luminous starburst galaxies tend to be more metal-poor, and therefore less dusty. These galaxies tend to be missed in IR surveys. The lowest SFRs in Fig. 2 ($\sim$1 $M_\odot$ yr^{-1}) correspond to the highest SFRs found in UV-selected starburst galaxies like blue compact dwarfs (see Heckman et al. 1998 for a compilation). Again, this is the direct consequence of emission-line or UV continuum surveys preferentially selecting more metal-poor, and therefore less luminous galaxies.

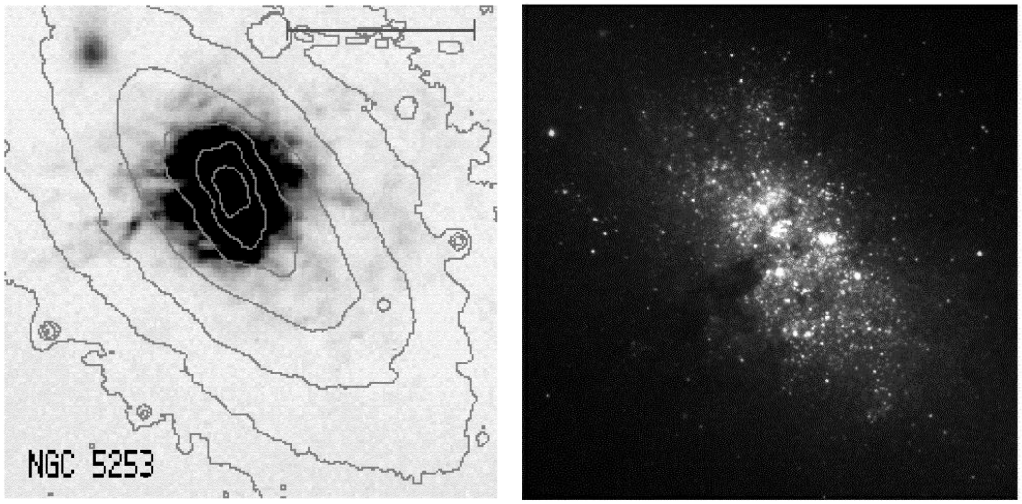

Figure 3. Left: Ground-based gray-scale Hα image of NGC 5253. The bar indicates a size of about 1 kpc. Overlaid are B contours (Marlowe et al. 1997). Right: Three-color (2600 Å, 5500 Å, 8000 Å) HST WFPC2 image of NGC 5253. The image has the same orientation as the ground-based image on the left. Field size is 1 kpc by 1 kpc (Calzetti et al. 1997).

Fig. 2 suggests that the highest star formation rates are found in the largest starburst regions, as measured by the extent of the Hα emitting region. Meurer et al. (1997) studied the integrated bolometric effective surface brightness of starbursts in the rest-frame UV, in the far-IR and Hα, and in the 21 cm radio continuum emission. Their sample is a combination of local starburst galaxies and several Lyman-break galaxies observed at cosmological redshift. The starburst intensity per unit surface area turns out to obey a well defined relation. Almost all galaxies are below a certain threshold over $2-3$ decades in starburst sizes. At the low end of the size distribution, the sample includes massive super star clusters with pc-scale sizes, and at the high end there are IR-luminous galaxies whose starburst regions extend over more than a kpc. 90% of the galaxies have normalized luminosities below $L_{\rm max} = 2 \times 10^{11}$ L$_\odot$ kpc^{-2}, with little dependence on starburst size and no evolution with redshift. Meurer et al. argue that this limit indicates a physical mechanism limiting the starburst intensity both for low- and for high-luminosity starbursts.

3. Detailed Morphology: pc Scale

Global starburst properties, while illuminating and useful for putting starburst galaxies into perspective, may be misleading for an understanding of the physics of the star formation process. As emphasized before, high gas densities do not automatically induce star formation. Depending on the turbulence compression, many dense cloud cores may in fact be stable and never form stars. In general, high gas densities lead to high gas pressure, and therefore to a high likelihood

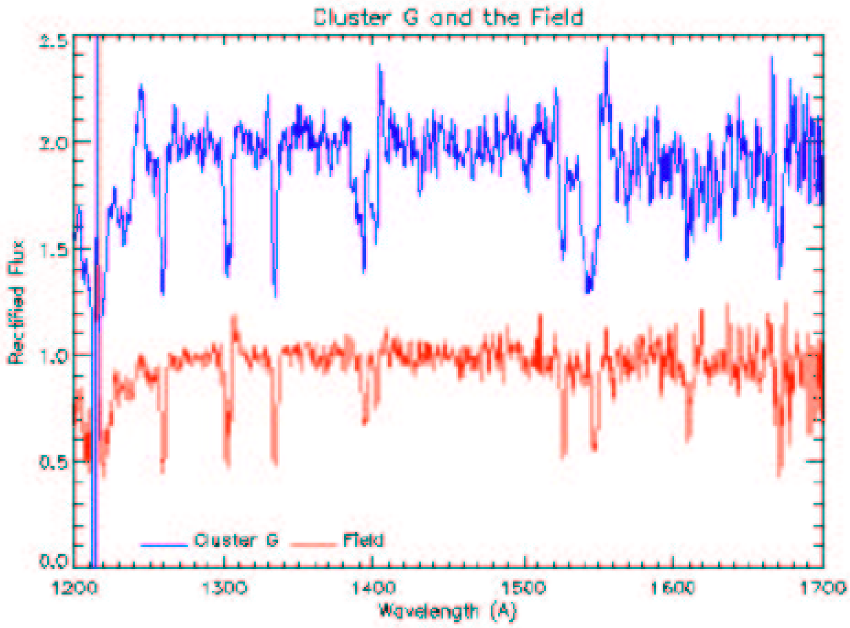

Figure 4. HST UV spectra of cluster G (upper) and of the diffuse field (lower) in NGC 5253 (Tremonti et al. 2001).

of induced or spontaneous star formation on a crossing time scale (Elmegreen 2000). Observations of starburst regions at high spatial resolution do indeed provide evidence for subtle sub-structure. Star formation rates vary in time and space over scales of tens of Myr and tens of pc, respectively.

The nearby blue amorphous dwarf galaxy NGC 5253 is an ideal laboratory to investigate starbursts down to pc sizes. At a distance of 3.3 Mpc (Tremonti et al. 2001), HST is capable of resolving structures as small as 1 pc. Although the outer regions of this galaxy are reminiscent of those in dwarf elliptical galaxies, star formation is active in the central kpc, as characterized by a high continuum surface brightness and strong Hα emission. Ground-based images by Marlowe et al. (1997) reproduced in Fig. 3 show emission filaments with sizes on the order of 1 kpc, comparable to the total galaxy size as given by the diameter of the blue isophotes. The Hα luminosity within the central 2 by 2 kpc is 2.8×10^{40} L$_\odot$, suggesting an average star formation rate of 0.1 M$_\odot$ yr^{-1}.

The right-hand panel of Fig. 3 is a multi-color HST image of the central 1 kpc of NGC 5253 (Calzetti et al. 1997). The starburst is resolved into multiple clusters with sizes, masses, and ages of $1-5$ pc, 10^4-10^5 M$_\odot$, and tens of Myr, respectively. The two youngest clusters alone account for about half of the observed Hα emission. Star formation has been active for at least 100 Myr, with significant intensity variations at different locations in the central region.

Spectra of individual clusters and of the diffuse field in NGC 5253 were obtained by Tremonti et al. (2001). Their UV spectrum of a typical cluster is contrasted with the mean field spectrum in Fig. 4. The spectral region between 1200 Å and 2000 Å shows stellar-wind lines of, e.g., C IV λ1550 and Si IV λ1400, which are the strongest features of hot stars in a young population (Leitherer et al. 1995; 2001). Hot-star winds are radiatively driven, with radiative momentum being transferred into kinetic momentum via absorption in metal lines, like those observed in the satellite-UV. Since the stellar far-UV radiation field depends on the proportion of the most massive, ionizing stars, changes in the IMF and/or the age of the population can be measured as changes in the line profiles. The two spectra in Fig. 4 are quite different. The cluster spectrum is characteristic of a single population with an age of a few Myr and containing massive stars up to $\sim$100 $M_\odot$. In contrast, the field spectrum has weak Si IV λ1400 and C IV λ1550, suggesting a deficit of very massive stars. Tremonti et al. interpret the difference as due to cluster evaporation in combination with the short life times of massive stars. The short relaxation times due to the compactness of the clusters and the strong tidal fields in the center of NGC 5253 lead to their rapid evaporation. After cluster evaporation, the remaining less massive stars will be part of the surrounding field population (Kim et al. 1999). This process can become the dominant effect governing the morphological evolution of a starbursts located in galaxy centers.

In most cases, spatial resolution limitations and, more importantly, dust obscuration preclude detailed morphological studies such as those of NGC 5253. As a cautionary example, I will discuss the case of NGC 7714. This is an SBb galaxy with a compact starburst in its nucleus. Weedman et al. (1981) interpreted its IUE UV spectrum as due to a massive star population and considered NGC 7714 as the proto-typical starburst nucleus. Lançon et al. (2001) analyzed UV-optical-IR spectra through matching 2$''$ (250 pc) apertures, together with HST and ground-based imagery. Due to its young age (of order 10^7 yr), the starburst nucleus is rich in ionizing O stars. The Lyman continuum luminosity is 10^{53} photons s^{-1}, which is about 10 times the output of 30 Dor in the LMC. The starburst is extended and has been proceeding for a period that is comparable to the lifetime of the massive stars. Therefore, red supergiants (RSG), the evolved descendants of O stars are observed in the red and IR as well. Analysis of the individual populations suggests that the RSG population seen in the IR is heavily obscured. The associated hot-star population would be 10 times more luminous than the actually observed, *dereddened* population at 1500 Å. In other words, even after reddening correction, the observed UV flux accounts for only about 10% of the actual luminosity — 90% of the UV light is totally hidden from view. The high-resolution HST images provide clues for understanding the apparent contradiction: the starburst nucleus of NGC 7714 is a group of clusters, each having different dust obscuration and brightness. Just one unobscured cluster accounts for the UV light in the HST aperture, whereas the sources responsible for the bolometric starburst luminosity are mostly hidden from the UV view. The decomposition of the optical-to-IR light also indicates that the youngest OB stars are *not* the dominant light source in the optical.

The properties of the central starburst in NGC 7714 help understand the long-standing puzzle of the discrepancy between observed and theoretically predicted recombination line equivalent widths in emission-line galaxies. The observed equivalent widths of, e.g., Hα and Hβ are typically less than half the theoretical prediction (e.g., Stasińska et al. 2001). Assuming the models can be trusted, this deficit could be interpreted as due to photon escape and/or continuum dilution. In the case of NGC 7714, the latter effect dominates. A comprehensive study of the stellar population in blue compact dwarf galaxies by

Mas-Hesse & Kunth (1999) indicates that NGC 7714 may not be the exception but rather the rule: in almost all cases the observed optical continuum shows an additional contribution from a population not seen in the UV light.

The lessons learned from NGC 7714 are manifold. Even a case of a spatially confined nuclear starburst turns out to have a complex star formation history with significant variations over tens to hundreds of Myr. The starburst is not an instantaneous event, nor is it a smooth continuous process over scales of hundreds of pc. Given the this complexity, it would be optimistic to believe we could determine star formation rates to better than a factor of 3, except in a few favorable cases.

4. Dust Obscuration, Attenuation, Absorption

A major complication for the interpretation of starburst galaxies in the UV and optical is the potentially large uncertainty introduced by dust obscuration. Starbursts are associated with the largest molecular gas densities (recall Fig. 1). This immediately suggests that dust must be plentiful since molecular hydrogen forms by adsorption on dust grains. Moreover, star formation comes together with metal production. Therefore the starburst itself will rapidly enrich the ISM in heavy elements and dust. This occurs over rather short time scales. The time scales for the formation of dust are only a few hundred Myr (Dwek 1998), so that obscuration effects can set in fairly early in the history of a galaxy.

Dust efficiently scatters and absorbs UV radiation. In order to quantify the interaction between dust and photons, assumptions on the amount of dust must be made, as well as on its geometry and chemical composition. Before discussing some pertinent result, I will clarify three definitions. (i) Dust *obscures* matter, i.e., dust conceals stars and gas from view by covering it wholly or in part. (ii) Dust *attenuates* light, i.e., it lessens the amount of light seen by an observer. This leaves open the possibility of either absorption or scattering. The wavelength dependence of the attenuation is often referred to as the *extinction law.* (iii) Dust *absorbs* photons, i.e., it transforms energy into a different form. The relevance of these definitions becomes obvious by recalling that in the Local Group the UV extinction law varies from galaxy to galaxy and within galaxies and is derived from observations of stellar point sources. The extinction is due to a combination of absorption and scattering of photons. The geometry is quite different in more distant galaxies where individual stars cannot be isolated. In such cases much of the light may be scattered into the line of sight, and the properties of the dust become paramount for the interpretation of the observed photon distribution (Meurer et al. 1999).

Fig. 5 (from Calzetti 2000) illustrates how dust attenuation corrections depend on the assumed dust properties. The various curves are the theoretically predicted relations between the dust attenuation measured in the optical (as expressed by $A_{\mathrm{H}\alpha}$ or τ_{V}) and the Hα/2800 Å luminosity ratio relative to the dust-free case. The considered geometries are for a homogeneous screen (identical to the standard Milky Way extinction law), a scattering homogeneous shell, a clumpy shell, a homogeneous spheroid, a homogeneous disk, and the starburst obscuration law of Calzetti et al. (2000). Clearly, the dust geometry has a major effect on the derived attenuation corrections. The empirically derived starburst

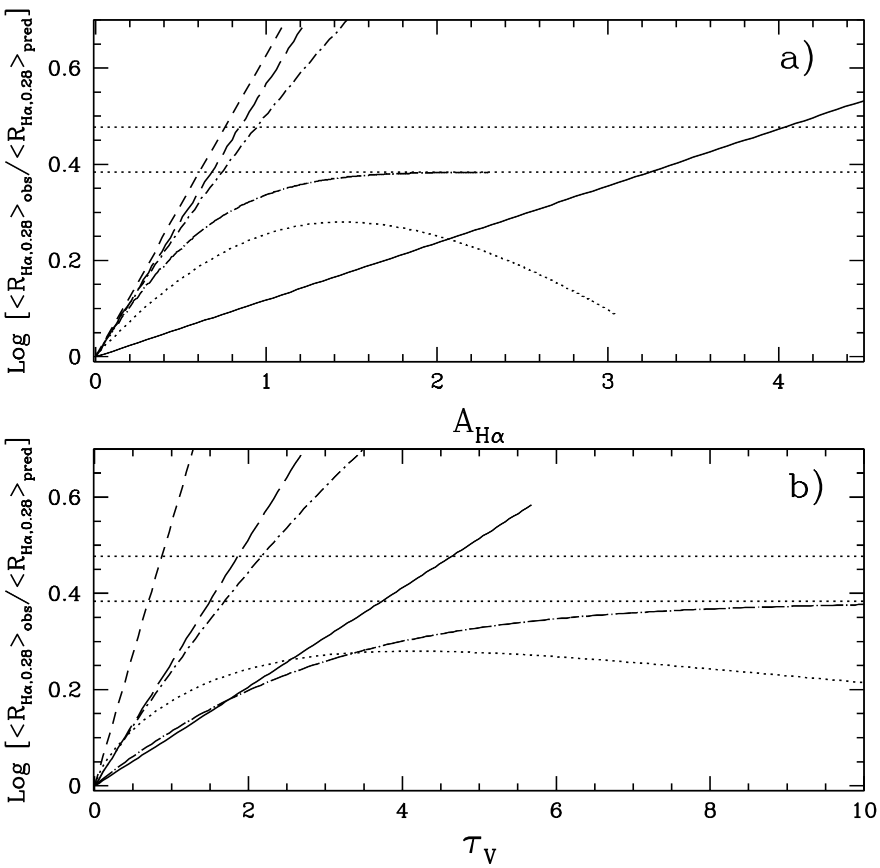

Figure 5. Relation between the observed and the predicted luminosity ratios at Hα and 2800 Å and the dust attenuation for various dust geometries. Upper panel: effective attenuation at Hα as abscissae; lower panel: optical depth in the V band. The curves are for a homogeneous screen (short-dashed), a scattering homogeneous shell (long-dashed), a clumpy shell (short-dash-dotted), a homogeneous spheroid (long-dash-dotted), a homogeneous disk (dotted), and the starburst obscuration law (solid). From Calzetti (2000).

obscuration law of Calzetti et al. is the "grayest" of the models in Fig. 5, i.e. it has the most gradual rise from the optical to the UV. In the local universe, UV/optically selected starburst galaxies are found to have average attenuation factors of $\sim$5 at 1500 Å when the empirical starburst obscuration law is applied.

Since the UV spectral region is close to the luminosity peak of a dust-free starburst population, an attenuation factor of 5 implies that 80% of the photons are absorbed and re-radiated in the far-IR if scattering is not important. Therefore a comparison between far-IR/UV luminosity ratio and the UV reddening allows one to test various dust geometries. This is shown in Fig. 6 (from Baker et al. 2001; based on Meurer et al. 1999). Since the far-IR flux is due to dust radiatively heated by the absorbed UV radiation, the y-axis is a measurement of dust absorption. The figure suggests a correlation between dust absorption and

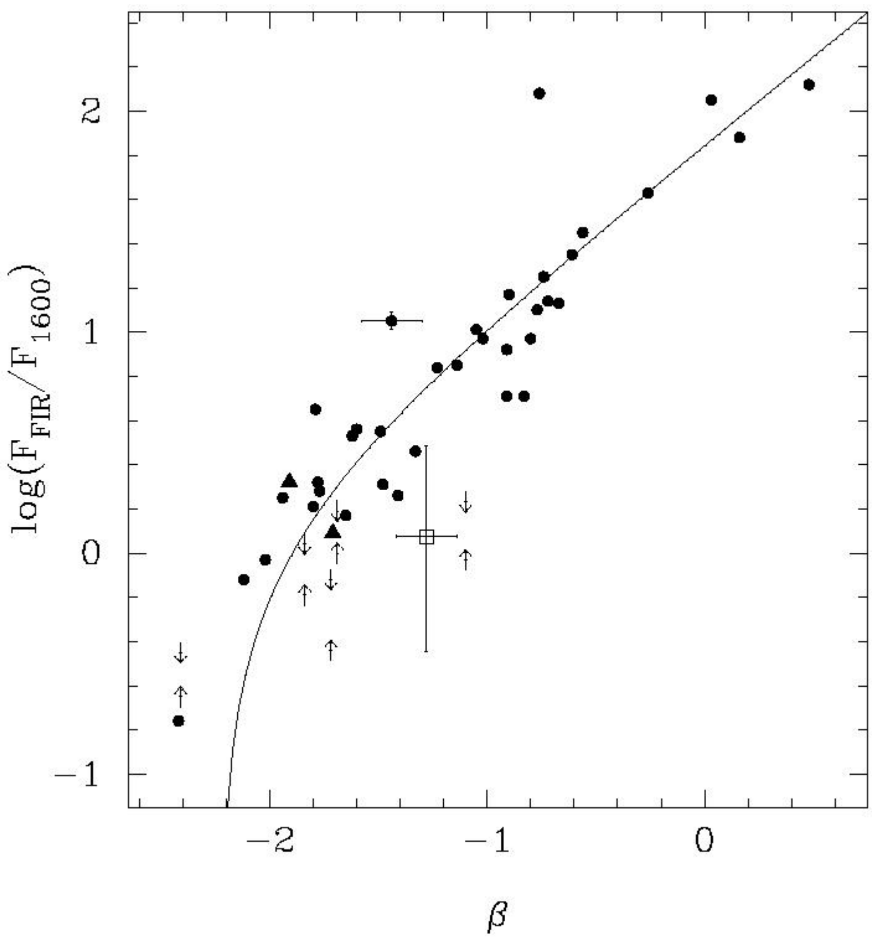

Figure 6. Ratio of the far-IR over UV luminosity vs. the UV spectral slope β. Various symbols: local starburst galaxies; open square with error bars: cB58; solid curve: empirical relation of Meurer et al. (1999). From Baker et al. (2001).

UV reddening. Such a relationship is expected for dust predominantly located in a foreground screen, possibly with inhomogeneities.

The significance of this relation becomes clear when starbursts at cosmological distance are included. If they have stellar and dust properties similar to those of their local far-IR selected counterparts, Fig. 6 can be used to *predict* the far-IR fluxes of high-redshift starbursts from their observed restframe UV reddening. So far, this test could only be done for one object since the expected flux levels are low. Baker et al. (2001; see also Sawicki 2001) reported a detection of the lensed galaxy cB58 at a redshift of $z = 2.7$. Their measurement is included in Fig. 6. The interpretation is ambiguous. cB58 is below the mean relation at the 1σ level, suggesting its far-IR luminosity is below the expectation. Verification of the applicability of the local far-IR/UV relation to cosmological distances must await detection of further high-z starbursts. Should the local

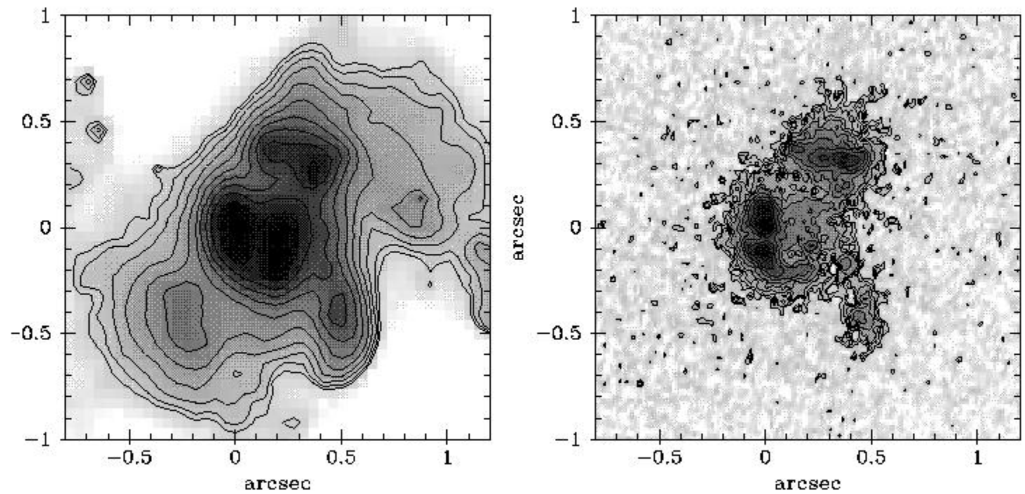

Figure 7. Central $2'' \times 2''$ (620×620 pc) of NGC 7130 in optical (left) and UV (right) light. From González Delgado et al. (1998).

relation be valid universally, dust-obscured starbursts could account for a substantial fraction of the cosmic far-IR background detected by the FIRAS and DIRBE experiments on the COBE satellite (Hauser et al. 1998).

5. Empirical Evidence For Starbursts Around AGNs

Simple energy considerations suggest the possibility of a connection between the starburst and the AGN phenomenon:

- The inferred accretion rates in Seyfert2 galaxies such as NGC 1068 are on the order of 0.1 $M_\odot$ yr^{-1} (Veilleux 2001). This is close to the star formation rate in a typical starburst galaxy like M82. Infall of gas to the galaxy center could feed both a starburst and an AGN.

- The bolometric luminosity functions of both starbursts and AGNs in the local universe are rather similar, at least where they are well determined (Soifer et al. 1987).

- The energy production over a Hubble time of both AGN and starbursts (as traced by the associated metal production) agree within the uncertainties (Heckman 1991).

There are strong theoretical arguments in favor of accretion as the powering source of AGNs. On the other hand, circumnuclear starbursts can have bolometric luminosities that rival even powerful QSOs (Sanders & Mirabel 1996). The close connection between starbursts and AGN has often been emphasized (e.g., Terlevich 1994) but observational proof has remained elusive until very recently. It was largely HST's spatial resolution and UV sensitivity which could unambiguously establish the existence of powerful starbursts in some AGNs.

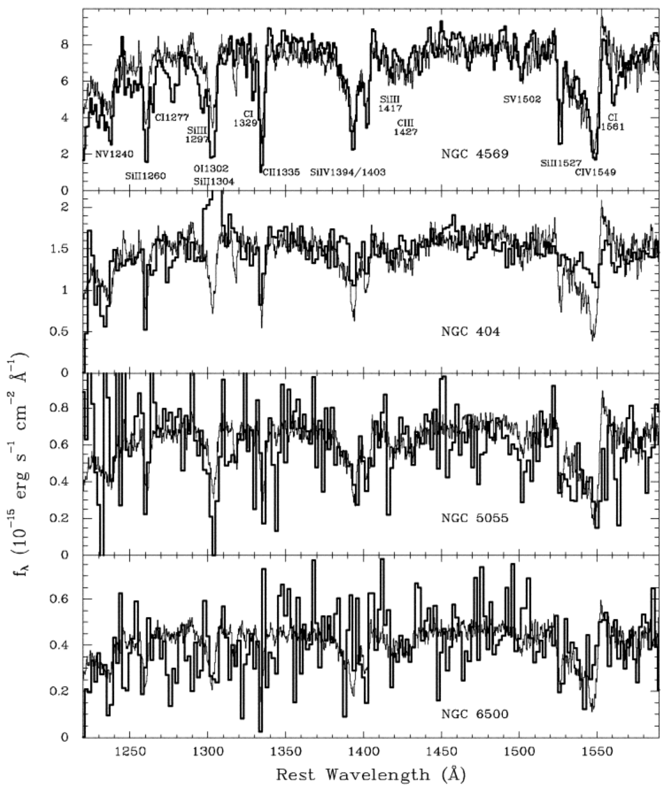

Figure 8. HST spectra of the four LINERs (heavy lines). Overlaid in each case is the spectrum of the starburst galaxy NGC 1741. From Maoz et al. (1998).

An example of some recent results is shown in Fig. 7. HST WFPC2 and FOC 2200 Å imaging of a sample of UV-bright Seyfert2 galaxies was done by González Delgado et al. (1998). Among them is NGC 7130, a UV-bright Seyfert2 galaxy. The 2200 Å passband contains no strong nebular emission lines and traces the stellar continuum of the recently formed OB stars. The nucleus, which was previously thought to be point-like, displays a complex morphology, suggestive of a circumnuclear starburst ring. Follow-up spectroscopy confirmed that the UV and optical light in the central 500 pc of NGC 7130 (and other program galaxies) is entirely dominated by star light and not by emission associated with the AGN.

A related study was performed by Maoz et al. (1998) who compared HST UV spectra of UV-bright LINERs. Massive, hot stars have few strong spectral features in the optical and near-IR so that their presence is easily hidden by a strong non-stellar continuum and by emission lines. The situation changes in the UV, where hot stars have unique, broad Si IV λ1400 and C IV λ1550 features. The spectra obtained by Maoz et al. are reproduced in Fig. 8 and compared to the spectrum of the starburst galaxy NGC 1741. There are clear absorption-line signatures of massive stars, indicating a stellar origin for the UV continuum. The similarity between NGC 4569 and NGC 1741 is particularly striking. The

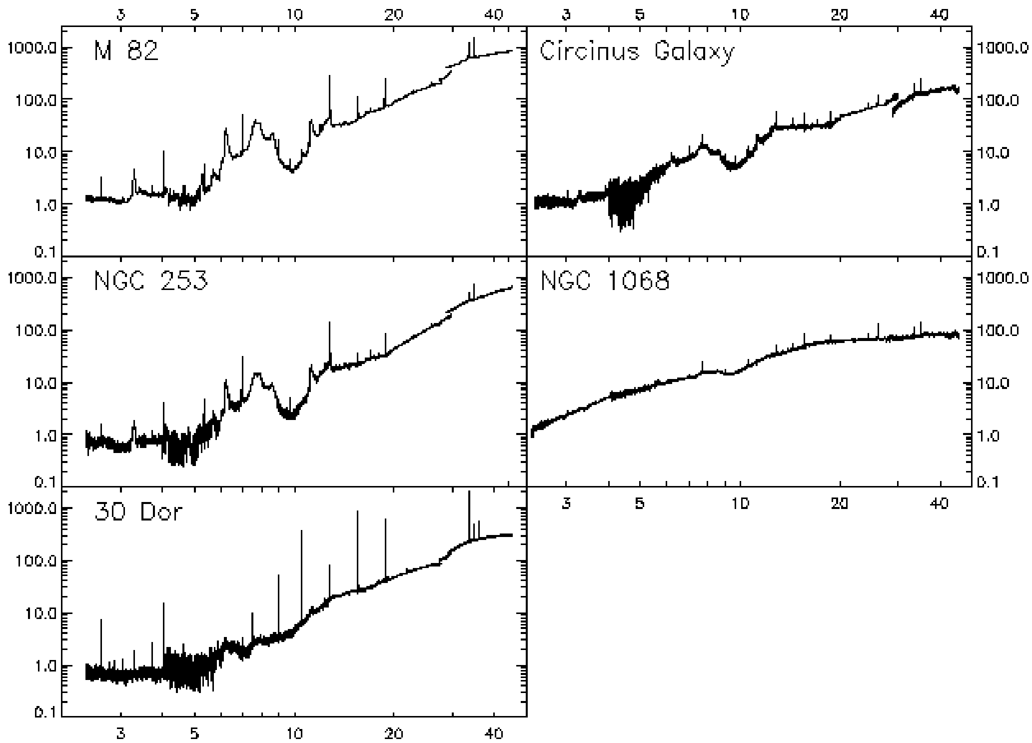

Figure 9. ISO SWS spectra of the starburst galaxies M82 and NGC 253, the giant H II region 30 Doradus, and the Seyfert2 galaxies Circinus and NGC 1068. From Sturm et al. (2000).

compact central UV continuum source that is observed in these galaxies is a nuclear star cluster rather than a low-luminosity AGN. Clearly these results must not be generalized; the sample was deliberately chosen to maximize the detection probability of hot stars. Nevertheless, the HST data are convincing evidence for the ubiquity of starbursts in AGN and their energetic significance in some cases.

6. Starbursts versus AGNs: the ISO Perspective

HST UV spectroscopy directly shows that hot stars provide most of the UV light in about 50% of the brightest type 2 Seyfert nuclei and UV-bright LINERs. The population of hot stars in these AGN is typically obscured and reddened by dust, with attenuation factors of 5 – 10 at 1500 Å. The implied UV luminosities of the starbursts range from $10^8 - 10^9$ $L_\odot$ in LINERs and $10^{10} - 10^{11}$ $L_\odot$ in type 2 Seyferts. Massive stars are energetically significant in these AGN (Heckman 1999). However, very few AGN could be studied with this technique, and these are biased in favor of cases with high UV surface brightness. Cid Fernandes et al. (2001) extended previous searches for stellar signatures in AGN by examining more easily measured quantities, such as equivalent widths of optical absorption lines, continuum colors , emission-line equivalent widths and profiles, far-IR luminosities, and near-UV surface brightness. Their larger sample and detailed semi-empirical population synthesis model puts earlier statistics on the occurrence of starbursts in AGN on a much more solid footing. 15 of 35 Seyfert2 galaxies are found to have composite starburst+AGN spectra. This is consistent with the previous UV-only results.

Analysis of stellar features is often preferable over nebular diagnostics, which can often be degenerate. A case in point are attempts to interpret the emission-line spectra of LINERs in terms of an ionizing stellar radiation field. Shields (1992) demonstrated that the general characteristics of LINERs can be generated via photoionization by relatively hot yet normal main-sequence O stars. His calculation results show improved agreement with observed LINER properties if the irradiated plasma is relatively dense and characterized by solar abundances modified by normal grain depletion. Such dense circumstellar media may be a natural consequence of high interstellar pressures, which may explain the preference of LINER phenomena for the nuclei of large and early-type galaxies.

Alternatively, Taniguchi et al. (2000) proposed an identification of some LINERs as post-starburst galaxies. In the post-starburst model, the ionization sources are planetary nebula nuclei (PNNs) with temperatures of ~100,000 K that appear in the evolution of intermediate-mass stars with mass between 3 and 6 $M_\odot$. The PNN phase lasts until the death of the least-massive stars formed in the starburst, which is about 5×10^8 yr for a stellar IMF truncated at 3 $M_\odot$.

Photoionization models of optical emission lines are plagued by this degeneracy: a carefully fine-tuned starburst spectrum can often mimic the same nebular emission line spectrum as does a power law spectrum from an AGN. An important result of the ISO mission (Genzel & Cesarsky 2000) was a set of mid-IR diagnostics which can break the degeneracy. Fig. 9 shows representative ISO SWS spectra of 30 Doradus (a giant H II region), M82 and NGC 253 (pure starbursts), and NGC 1068 and the Circinus galaxy (two Seyfert2 galaxies with circumnuclear starbursts). The differences between the spectra are striking. The starbursts and 30 Doradus have strong low-excitation fine structure lines, few and/or weak high-excitation lines, little dust emission below 10 μm, and very strong PAH bands. PAHs (= polycyclic aromatic hydrocarbon) are large carbon molecules formed in dense, neutral interstellar clouds. In contrast, the two Seyfert2 galaxies have fainter emission lines, but with much higher excitation (e.g., the much stronger [O IV] 25.9 μm line). The dust continuum is much stronger in the AGN-type spectra. Note that NGC 1068 and the Circinus galaxy both have circumnuclear starbursts. Therefore they show starburst features as well.

Diagnostic diagrams are powerful tools for an empirical characterization of the excitation state of a source. Genzel et al. (1998) introduced the [O IV] 25.9 μm to [Ne II] 12.8 μm line flux ratio versus the strength of the PAH bands to discriminate between starbursts and AGN. Fig. 10 demonstrates that this ISO diagnostic diagram clearly separates known star forming galaxies from AGNs. The diagram is insensitive to dust extinction if the emission lines and the bands are affected by a similar amount of extinction. [O IV], although weak, is often

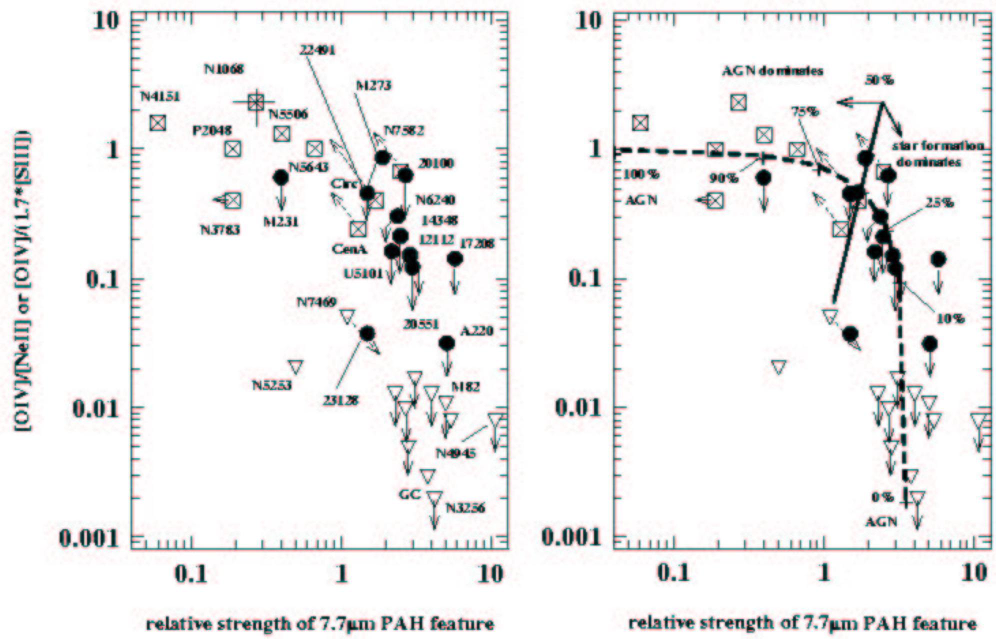

Figure 10. Diagnostic diagram showing the [O IV]/[Ne II] line ratio vs. the strength of the 7.7 μm PAH feature. Starburst galaxies: open triangles; ULIRGs: filled circles; AGN: crossed rectangles. Left: basic data with individual sources marked. Right: simple linear mixing curve, made by combining various fractions of total luminosity in an AGN and a starburst. From Genzel et al. (1998).

detected in starburst galaxies (Lutz et al. 1998). Its origin is not yet completely understood. Fast, ionizing shocks powered by supernovae and stellar winds have been considered by Viegas et al. (1999). In addition, hot Wolf-Rayet stars can meet the ionization budget in some galaxies as well (Crowther et al. 1999; Schaerer & Stasińska 1999).

The diagnostic diagram in Fig. 10 is most powerful when applied to dusty, IR-luminous galaxies, where the nature of the underlying source is not known a priori. ULIRGs in particular are objects of interest, as the starburst versus AGN debate is still ongoing (Sanders & Mirabel 1996). Genzel et al. (1998) studied 13 ULIRGs and found that the AGN is only dominant in four objects. The sample can be extended by relying on the PAH strength alone (see Genzel & Cesarsky 2000 for a discussion). Starbursts dominate up to luminosities of about 2×10^{12} L$_\odot$, above which AGN become energetically more and more important. The most luminous starbursts are detected in galaxies with luminosities close to $\sim 10^{13}$ L$_\odot$. This limit corresponds to the maximum star formation rate of $\sim 10^3$ M$_\odot$ yr^{-1} of a gas-rich spheroid undergoing a monolithic collapse on a dynamical time scale.

There is now ubiquitous evidence for starbursts in AGN over several decades in luminosity. While the precise evolutionary scheme is still unknown, it seems likely that the gas supply feeding the central AGN is capable if sustaining the circumnuclear starburst as well.

References

Baker, A. J., Lutz, D., Genzel, R., Tacconi, L. J., & Lehnert, M. D. 2001, A&A, in press

Balzano, V. A. 1983, ApJ, 268, 602

Calzetti, D. 2000, in Building Galaxies: From the Primordial Universe to the Present, ed. F. Hammer, T. X. Thuan, V. Cayatte, B. Guiderdoni, & J. T. T. Van (Singapore: World Scientific), 233

Calzetti, D., Armus, L., Bohlin, R. C., Kinney, A. L., Koornneef, J., & Storchi-Bergmann, T. 2000, ApJ, 533, 682

Calzetti, D., Meurer, G. R., Bohlin, R. C., Garnett, D. R., Kinney, A. L., Leitherer, C., & Storchi-Bergmann, T. 1997, AJ, 114, 1834

Cid Fernandes, R., Heckman, T. M., Schmitt, H., González Delgado, R. M., & Storchi-Bergmann, T. 2001, ApJ, in press

Crowther, P. A., Beck, S. C.. Willis, A. J., Conti, P. S., Morris, P. W., & Sutherland, R. S. 1999, MNRAS, 304, 654

Dwek, E. 1998, ApJ, 501, 643

Elmegreen, B. G. 1999, in Star Formation 1999, ed. T. Nakamoto (Nobeyama Radio Observatory), 3

Elmegreen, B. G., 2000, ApJ, 530, 277

Genzel, R., & Cesarsky, C. J. 2000, ARA&A, 38, 761

Genzel, R., Lutz, D., Sturm, E., Egami, E., Kunze, D., Moorwood, A. F. M., Rigopoulou, D., Spoon, H. W. W., Sternberg, A., Tacconi-Garman, L. E., Tacconi, L., & Thatte, N. 1998, ApJ, 498, 579

González Delgado, R. M., Heckman, T. M., Leitherer, C., Meurer, G. R., Krolik, J., Wilson, A. S., Kinney, A. L., & Koratkar, A. 1998, ApJ, 505, 174

Hauser, M. G., et al. 1998, ApJ, 508, 25

Heckman, T. M. 1991, in Massive Stars in Starbursts, ed. C. Leitherer, N. R. Walborn, T. M. Heckman, & C. A. Norman (Cambridge: CUP), 289

——. 1997, in Star Formation Near and Far, ed. S. S. Holt & L. G. Mundy (Woodbury: AIP), 393, 271

——. 1999, in IAU Symp 193, Wolf-Rayet Phenomena in Massive Stars and Starburst Galaxies, ed. K. A. van der Hucht, G. Koenigsberger, & P. R. J. Eenens (San Francisco: PASP), 703

Heckman, T. M., Robert, C., Leitherer, C., Garnett, D. R., & van der Rydt, F. 1998, ApJ, 503, 646

Kennicutt, R. C. 1998, ApJ, 498, 541

Kim, S. S., Morris, M., & Lee, H. M. 1999, ApJ, 525, 228

Lançon, A., Goldader, J. D., Leitherer, C., & González Delgado, R. M. 2001, ApJ, 552, 150

Lehnert, M. D., & Heckman. T. M. 1996, ApJ, 472, 546

Leitherer, C., Leão, J. R. S., Heckman, T. M., Lennon, D. J., Pettini, M., & Robert, C. 2001, ApJ, 550, 724

Leitherer, C., Robert, C., & Heckman, T. M. 1995, ApJS, 99, 173

Leitherer, C., Schaerer, D., Goldader, J. D., González-Delgado, R. M., Robert, C., Foo Kune, D., de Mello, D. F., Devost, D., & Heckman, T. M. 1999, ApJS, 123, 3

Lutz, D., Kunze, D., Spoon, H. W. W., & Thornley, M. D. 1998, A&A, 333, 75

Lynds, C. R., & Sandage, A. R. 1963, ApJ, 137, 1005

Maoz, D., Koratkar, A., Shields, J. C., Ho, L. C., Filippenko, A. V., & Sternberg, A. 1998, AJ, 116, 55

Marlowe, A. T., Meurer, G. R., Heckman, T. M., & Schommer, R. 1997, ApJS, 112, 285

Martin, C. L., & Kennicutt, R. C. 2001, ApJ, in press

Mas-Hesse, M., & Kunth, D. 1999, A&A, 349, 765

Meurer, G. R., Heckman, T. M., & Calzetti, D. 1999, ApJ, 521, 64

Meurer, G. R., Heckman, T. M., Leitherer, C., Lehnert, M., & Lowenthal, J. 1997, AJ, 114, 54

Mihos, J. C., & Hernquist, L. 1996, ApJ, 464, 641

Rieke, G. H. 1991, in Massive Stars in Starbursts, ed. C. Leitherer, N. R. Walborn, T. M. Heckman, & C. A. Norman (Cambridge: CUP), 285

Rieke, G. H., & Low, F. J. 1975, ApJ, 197, 17

Sanders, D. B. 1997, in Starburst Activity in Galaxies, ed. J. Franco, R. Terlevich, & A. Serano, Rev. Mex. Astron. Astrofis. Conf. Ser., 6, 42

Sanders, D. B., & Mirabel, I. F. 1996, ARA&A, 34, 749

Sawicki, M. 2001, AJ, 121, 2405

Schaerer, D., & Stasińska, G. 1999, A&A, 345, L17

Schmidt, M. 1959, ApJ, 129, 243

Shields, J. C. 1992, ApJ, 399, L27

Soifer, B. T., Sanders, D. B., Madore, B. F., Neugebauer, G., Danielson, G. E., Elias, J. H., Lonsdale, C. J., & Rice, W. L. 1987, ApJ, 320, 238

Stasińska, G., Schaerer, D., & Leitherer, C. 2001, A&A, 370, 1

Sturm, E., Lutz, D., Tran, D., Feuchtgruber, H., Genzel, R., Kunze, D., Moorwood, A. F. M., & Thornley, M. D. 2000, A&A, 358, 481

Taniguchi, Y., Shioya, Y., & Murayama, T. 2000, AJ, 120, 1265

Terlevich, R. 1994, in Violent Star Formation, ed. G. Tenorio-Tagle (Cambridge: CUP), 329

Terlevich, R., Melnick, J., Masegosa, J., Moles, M., & Copetti, M. V. F. 1991, A&AS, 91, 285

Tinsley, B. M., & Larson, R. B. 1978, ApJ, 221, 554

Tremonti, C. A., Calzetti, D., Heckman, T. M., & Leitherer, C. 2001, ApJ, in press

Veilleux, S., in Starbursts: Near and Far, ed. L. J. Tacconi & D. Lutz (Berlin: Springer), in press

Viegas, S. M., Contini, M., & Contini, T. 1999, A&A, 347, 112

Weedman, D. W., Feldman, F. R., Balzano, V. A., Ramsey, L. W., Sramek, R. A., & Wu, C.-C. 1981, ApJ, 248, 105

Acknowledgments. Financial support from the conference organizers is gratefully acknowledged. Daniela Calzetti kindly provided an updated version of Fig. 5 and made several suggestions which improved an earlier version of the manuscript.